Engineering Science and Technology, an International Journal xxx (2016) xxx–xxx

HOSTED BY

ELSEVIER

Contents lists available at ScienceDirect

Engineering Science and Technology, an International Journal

journal homepage: www.elsevier.com/locate/jestch

Full Length Article

Series analysis for the flow between two stretchable disks

Vishwanath B. Awati [a,*], Manjunath Jyoti [a], K.V. Prasad [b]

[a] Department of Mathematics, Rani Channamma University, Belagavi 591 156, India
[b] Department of Mathematics, Vijayanagara Srikrishnadevaraya University, Bellary 583 104, India

ARTICLE INFO

Article history:
Received 9 September 2016
Revised 3 November 2016
Accepted 13 November 2016
Available online xxxx

Keywords:
Stretchable disks
Dirichlet series
CESS
Domb-Sykes plot
HAM and Pade' approximants
Residual error

ABSTRACT

In this paper, we present the semi-analytical/semi-numerical solution of an axis-symmetric flow between two coaxial infinite stretching disks. The governing momentum equations in cylindrical co-ordinates are reduced to fourth order nonlinear ordinary differential equation (NODE) with the relevant boundary conditions. The resulting nonlinear boundary value problem is solved by using Computer Extended Series Solution (CESS) and Homotopy Analysis Method (HAM). The effects of Reynolds number R and disk stretching parameter γ are discussed in detail. The resulting solutions are compared with the earlier numerical findings. The above methods admit a desired accuracy and the results are presented in the form of graphs. The validity of the series solution is extended to a much larger values of R up to infinity. Further, the variations of shear stress and pressure parameter as a functions of R and γ are analyzed. For very large R, the governing equation reduces to third order NODE with infinite boundary is solved by using Dirichlet series and the solution is compared with the numerical findings.

1. Introduction

The study of boundary layer flow of a viscous incompressible fluid over a moving boundary/stretching boundary has significant applications in engineering and industrial processes, such as plastic and metal industries involving surface stretching or extrusion processes [1–3]. Sakiadis [4,5] was the first researcher to propose the surface stretching problem based on boundary layer assumptions. According to Wang [6] it is not an exact solution of the Navier-Stokes (NS) equations. Crane [7] find an exact solution for the two dimensional stretching sheet problems, where the surface stretching velocity is proportional to the distance from the fixed slot. The generalization of Crane problem to a power law stretching velocity based on boundary layer flows discussed by Kukien [8] and Bank [9]. Gupta and Gupta [10] considered the Crane problem with mass injection/suction at the wall and Wang [11] studied the same problem in a rotating system. Wang [12] examined the three dimensional flow due to stretching flat surface. Brady and Acrivos [13] find another exact solution of NS equations involving the flow inside a channel or tube with a stretching wall. Wang [14] studied the flow outside an accelerating stretching tube, which was also demonstrated as an exact solution for the NS equations. The unsteady developments [15–17] and the spatial stability [18] of a class of similarity solutions for the Brady and Acrivos problem [13] were further studied. Zaturska and Bank [19] discussed the channel problem with combined effects of porous and stretching walls. Rasmussen [20] examined the steady viscous flow between porous disks with mass suction. Turkyilmazoglu [21–23], examined the MHD fluid flow and heat transfer, three dimensional MHD stagnation flow also discussed the flow and heat simultaneously induced due to a stretchable rotating disk. Mustafa et al. [24] analyzed on Bodewadt flow and heat transfer of nanofluids over a stretching stationary disk. Hayat and his collaborators [25–28] have discussed the various physical aspects of convection flow of carbon nanotubes with thermal radiation effects, partial slip effect and effects of homogeneous-heterogeneous reactions in flow of magnetic-Fe_3O_4 nanoparticles, and unsteady stagnation point flow of viscous fluid between rotating disks.

Recently Sheikholeslami and his associates [29–38] have examined the various semi-analytical methods such as DTM, ADM, HPM and OHAM for the solution of different types flow and heat transfer problems arise in fluid mechanics. In this paper, we present the series solution of the flow between two coaxial stretching disks for small and moderately large Reynolds numbers. In the first method, we investigate the flow problem based on a new type of series analysis (CESS) and present some interesting results. The salient features of this method are evidently explained by Van Dyke [39]. Bujurke and his associates [40–43] have clearly shown the potential applications of these methods in computational fluid dynamics. These methods reveal the analytical structure of the

* Corresponding author.
E-mail address: awati_vb@yahoo.com (V.B. Awati).
Peer review under responsibility of Karabuk University.

http://dx.doi.org/10.1016/j.jestch.2016.11.011
2215-0986/

Please cite this article in press as: V.B. Awati et al., Series analysis for the flow between two stretchable disks, Eng. Sci. Tech., Int. J. (2016), http://dx.doi.org/10.1016/j.jestch.2016.11.011

Nomenclature

d	distance between the disks	F, H	dimensionless stream functions
p	fluid pressure	η	similarity independent variable
r	radius of the disk	v	kinematic viscosity of the fluid ($m^2\ s^{-1}$)
E	disk stretching strength parameter	ρ	density of the fluid ($kg\ m^{-3}$)
R	Reynolds number	γ	disk stretching parameter
u_r, u_z	velocity components in the directions r and z respectively	β	pressure parameter

solution which is not clear in case of other methods. The few manually calculated perturbation solutions in the low Reynolds number of the boundary value problem which enables us to propose a systematic series expansion to generate large number of universal polynomial coefficients by using recurrence relation and Mathematica. The resulting series will be limited in convergence by nonphysical singularities are extended to moderately high Reynolds numbers using an analytic continuation of the series solution. The location and nature of the singularity which restricts the convergence of the series is predicted using Domb-Sykes plot [44]. The analytic continuation can be achieved by extend the validity of the perturbation series to moderately larger values of Reynolds number using Pade' approximants. For large R, the governing NODE is reduced to third NODE with infinite interval and for the solution of this equation we have used the Dirichlet series method.

We also investigate the same flow problem using fast converging semi-analytical method called Homotopy analysis method (HAM) proposed by Liao [45]. The HAM provides the solution in much convenient way, to adjust and control convergence region of the series. In this method we have the liberty to choose base functions of the required solution and the corresponding auxiliary linear operator. Therefore, the HAM has an excellent flexibility and generality over all other analytical or approximate methods and also it is easy to use. Awati et al. [46] discussed the solution of MHD flow of viscous fluid between two parallel porous plates using CESS and HAM. Most recently, Hayat and his research colleagues [47–59], have successfully analyzed different types of fluids in MHD flow problems and stretching surfaces which arise in the engineering and science fields using HAM.

The paper is structured as follows. Section 1 describes the introduction; Section 2 develops the mathematical formulation of the proposed problem with relevant boundary conditions. The solution of the problem is obtained by Computer extended series as well as Homotopy analysis method in Sections 3 and 4 respectively. Section 5 presents results and discussion; Section 6 is about the conclusion (see Table 1).

2. Mathematical formulation

Consider an axis-symmetric viscous flow between two coaxial infinite stretching disks with a distance d between them. The disks are stretched in the radial direction with the velocity proportional to the radii and the lower disk is placed at the plane $z = 0$. The schematic diagram for the considered flow problem phenomenon is given in Fig. 1.

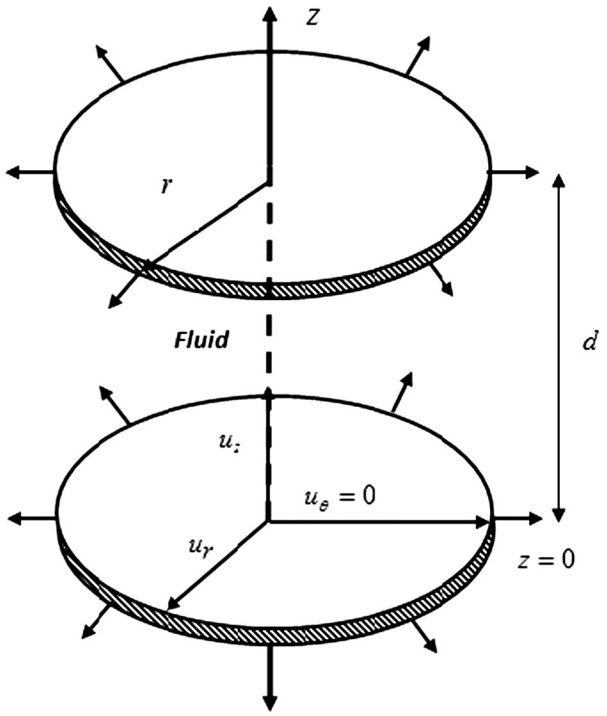

Fig. 1. Schematic diagram of the flow phenomenon.

For the viscous incompressible fluid in the absence of body forces and based on an axis-symmetry flow, the steady state NS equations in cylindrical polar coordinates [60] becomes

$$\frac{1}{r}\frac{\partial}{\partial r}(ru_r) + \frac{\partial u_z}{\partial z} = 0 \tag{2.1}$$

$$u_r\frac{\partial u_r}{\partial r} + u_z\frac{\partial u_r}{\partial z} = -\frac{1}{\rho}\frac{\partial p}{\partial r} + v\left(\frac{\partial^2 u_r}{\partial r^2} + \frac{1}{r}\frac{\partial u_r}{\partial r} + \frac{\partial^2 u_r}{\partial z^2} - \frac{u_r}{r^2}\right) \tag{2.2}$$

$$u_r\frac{\partial u_z}{\partial r} + u_z\frac{\partial u_z}{\partial z} = -\frac{1}{\rho}\frac{\partial p}{\partial z} + v\left(\frac{\partial^2 u_z}{\partial r^2} + \frac{1}{r}\frac{\partial u_z}{\partial r} + \frac{\partial^2 u_z}{\partial z^2}\right) \tag{2.3}$$

where $V = (u_r, u_z)$ is the velocity vector, v is the kinematic viscosity of the fluid, p be the pressure of the fluid and ρ is the density of the fluid. We use the following transformations [61] such as

Table 1
Comparison of shear stress at the surface $f''(0), f(\infty)$ by using Dirichlet series with numerical method [61].

Dirichlet series				Numerical [61]	
a	γ	$f''(0)$	$f(\infty)$	$f''(0)$	$f(\infty)$
1.13583860	−1.50299405	−2.347441	−1.50299405	−2.347442	−1.502996

Please cite this article in press as: V.B. Awati et al., Series analysis for the flow between two stretchable disks, Eng. Sci. Tech., Int. J. (2016), http://dx.doi.org/10.1016/j.jestch.2016.11.011

$$u_r = rEF(\eta), \quad u_z = EdH(\eta), \quad p = \rho E\nu\left[P(\eta) + \frac{1}{4}\beta r^2/d^2\right] \tag{2.4}$$

where E is the parameter corresponding to the disk stretching strength and $\eta = z/d$ is a similarity variable. Substituting Eq. (2.4) into Eqs. (2.1)-(2.3), we get

$$H' = -2F \tag{2.5}$$

$$F'' - \beta = R(F^2 + F'H) \tag{2.6}$$

$$P' = 2RFH - 2F' \tag{2.7}$$

with the relevant boundary conditions are

$$F(0) = 1, \quad H(0) = 0, \quad H(1) = 0, \quad F(1) = \gamma \text{ and } P(0) = 0 \tag{2.8}$$

where $R = Ed^2/\nu$ is the wall stretching Reynolds number proportional to the disk stretching strength and γ is the upper disk stretching parameter representing the velocity ratio of the upper disk to the lower disk. Without loss of generality, it is assumed that $0 \leqslant \gamma \leqslant 1$. For $\gamma > 1$, we normalize the flow problem by the upper disk and switch the coordinate direction. Substituting Eq. (2.5) into Eq. (2.6), we get

$$H''' + \beta - RHH'' + \frac{RH'2}{2} = 0 \tag{2.9}$$

and the boundary conditions take the forms

$$H(0) = 0, \quad H(1) = 0, \quad H'(0) = -2, \quad H'(1) = -2\gamma \tag{2.10}$$

Differentiating Eq. (2.9) with respect to η, we get

$$H'''' - RHH''' = 0 \tag{2.11}$$

The pressure parameter β can be obtained from Eq. (2.9) and (2.10) for putting $\eta = 0$, we get

$$\beta = -2R - H'''(0) \tag{2.12}$$

For large R: Let us define a new variable $\varepsilon = \sqrt{R}\eta$ and the corresponding new function $f(\varepsilon) = \sqrt{R}H(\eta)$, then substituting $f(\varepsilon)$ into Eq. (2.9), we get

$$Rf'''' + \beta - Rff'' + R\frac{f'2}{2} = 0 \tag{2.13}$$

with the appropriate boundary conditions are

$$f(0) = 0, \quad f(\sqrt{R}) = 0, \quad f'(0) = -2, \quad f'(\sqrt{R}) = -2\gamma \tag{2.14}$$

For large R, then the Eq. (2.9) becomes

$$f'''' - ff'' + \frac{1}{2}f'2 = 0 \tag{2.15}$$

For the above equation, when $R \to \infty$, the flow represents the boundary layer behavior near the wall, the fluid far from the wall and not affected by the wall. The associated boundary conditions becomes

$$f(0) = 0, \quad f'(0) = -2, \quad f'(\infty) = 0 \tag{2.16}$$

We seek Dirichlet series solution of Eq. (2.15) satisfying the derivative boundary conditions at infinity in the form

$$f(\eta) = -\gamma + \gamma\sum_{n=1}^{\infty} b_n a^n e^{-n\gamma\eta} \tag{2.17}$$

where the parameter $\gamma > 0$ and $|a| < 1$ are to be determined. Substituting Eq. (2.17) into Eq. (2.15), we get

$$-\sum_{n=1}^{\infty} n^3 b_n a^n e^{-n\gamma\eta} + \sum_{n=1}^{\infty} n^2 b_n a^n e^{-n\gamma\eta} - \sum_{n=2}^{\infty}\sum_{k=1}^{n-1} k^2 b_k b_{n-k} a^n e^{-n\gamma\eta} + \frac{1}{2}\sum_{n=2}^{\infty}\sum_{k=1}^{n-1} k(n-k) b_k b_{n-k} a^n e^{-n\gamma\eta} = 0 \tag{2.18}$$

To obtain b_n as functions of unknown parameters γ and a. For $n = 1$ in (2.18), we have the identity $-b_1 a + b_1 a = 0$. We write the above recurrence relation (2.18) in the form

$$b_n = \frac{1}{n^2(n-1)}\sum_{k=1}^{n-1}\left[-k^2 + \frac{1}{2}k(n-k)\right] b_k b_{n-k} \tag{2.20}$$

for $n = 1, 2, 3, \ldots$. If $|a| < 1$ and $|b_n| \leqslant 1$ then the series (2.17) converges absolutely for any $\gamma > 0$ and $\eta = -\varepsilon$, where

$$\varepsilon = -\left[\frac{\ln|a|}{\gamma} + \delta\right] > 0$$

and $\delta > 0$ is sufficiently small number depending on a and γ. The series converges absolutely and uniformly on the half axis $\eta > -\varepsilon$. A general convergence criterion of the Dirichlet series may be found in Riesz [62].

To obtain the shear stress at the surface $f''(0)$ as fallows

$$f''(0) = \gamma^2\sum_{n=1}^{\infty} b_n a^n (-n\gamma)^2 \tag{2.21}$$

The series (2.21) contains two unknown parameters a and γ are determined from the remaining boundary conditions (2.16) at $\eta = 0$; namely

$$f(0) = -\gamma + \gamma\sum_{n=1}^{\infty} b_n a^n = 0 \tag{2.22}$$

$$f'(0) = \gamma^2\sum_{n=1}^{\infty}(-n) b_n a^n = -2 \tag{2.23}$$

3. Series solution

We seek a perturbation solution of Eq. (2.11) in powers of R in the form

$$H(\eta) = \sum_{n=0}^{\infty} R^n H_n(\eta) \tag{3.24}$$

Substituting Eq. (3.24) into Eq. (2.11) and equating like powers of R on both sides, we get

$$H_0'''' = 0 \tag{3.25}$$

$$H_{n+1}'''' = H_0 H_n''' + H_n H_0''' + \sum_{L=1}^{n-1}[H_L H_m''''], \quad n = 1, 2, 3 \ldots \tag{3.26}$$

where $m = n - L$. The associated boundary conditions are

$$H_0(0) = 0, \quad H_0(1) = 0, \quad H_0'(0) = -2, \quad H_0'(1) = -2\gamma \tag{3.27}$$

$$H_n(0) = 0, \quad H_n(1) = 0, \quad H_n'(0) = 0, \quad H_n'(1) = 0, \quad n \geqslant 1 \tag{3.28}$$

The solutions of the above equations satisfying the boundary conditions are given by

$$H_0 = -2\eta + (4 + 2\gamma)\eta^2 - (2 + 2\gamma)\eta^3$$
$$H_1 = \frac{1}{105}\left[(12 + 3\gamma - 9\gamma^2)\eta^2 + (-22 - 9\gamma + 12\gamma^2)\eta^3 + (21 + 21\gamma)\eta^5 + (-14 - 21\gamma - 7\gamma^2)\eta^6 + (3 + 6\gamma + 3\gamma^2)\eta^7\right] \tag{3.29}$$

Please cite this article in press as: V.B. Awati et al., Series analysis for the flow between two stretchable disks, Eng. Sci. Tech., Int. J. (2016), http://dx.doi.org/10.1016/j.jestch.2016.11.011

$$H_2 = \frac{1}{727650}\begin{bmatrix} (498 - 1740\gamma - 354\gamma^2 + 1884\gamma^3)\eta^2 - (-3566 - 2777\gamma - 2777\gamma^2 + 3566\gamma^3)\eta^3 \\ +(15246 + 6237\gamma - 9009\gamma^2)\eta^5 + (-12936 - 12705\gamma + 5313\gamma^2 + 5082\gamma^3)\eta^6 \\ +(-16434 - 14652\gamma - 792\gamma^2 - 2574\gamma^3)\eta^7 + (34650 + 51975\gamma + 17325\gamma^2)\eta^8 \\ +(-24640 - 49280\gamma - 28490\gamma^2 - 3850\gamma^3)\eta^9 + \begin{pmatrix} 8316 + 20790\gamma + 16632\gamma^2 \\ +4158\gamma^3 \end{pmatrix}\eta^{10} \\ +(-1134 - 3402\gamma - 3402\gamma^2 - 1134\gamma^3)\eta^{11} \end{bmatrix}$$

3.1. Computer extended series

It is not sufficient to analyze the series (3.24) by using the above three terms of the series. We require sufficiently large number of terms (universal polynomial coefficients) to analyze the series to reveal the true nature of the solution representing the series. As we proceed for higher order terms, the algebra becomes cumbersome and it is difficult to perform this manually, but it can be made automatic using Mathematica. Based on the nature of solution functions (3.29), we are able to propose a systematic series expansion with universal polynomial coefficients which is quite useful and efficient in generating the higher order terms of the series. Towards this goal, we find a general form $H_n(\eta)$ to be of the form

$$H_n(\eta) = \sum_{k=2}^{4n+1} A_{(n,k)}\left[\eta^{(k+2)} - 2\eta^{(k+1)} + \eta^{k)}\right], \quad n = 1,2,3,\ldots \tag{3.30}$$

The above expression generates exactly the earlier calculated approximations H_i for $(i = 1,2)$. Using the following recurrence relation and Mathematica we can generate H_i for $(i > 2)$. Substitute Eq. (3.30) into Eq. (3.26) and equate various powers of η on both sides and obtain a recurrence relation for generating the unknown coefficients $A_{n,k}$ in the form

$$A_{(n+1,4n-J)} = 2A_{(n+1,4n-(J-1))} - A_{(n+1,4n-(J-2))} + \frac{1}{(4n-(J-2))(4n-(J-1))(4n-J)(4n-(J+1))}$$

$$\times\left\{\sum_{i=1}^{5} A_{(n,k)}S_i(k) + \sum_{L=1}^{n-1}\Bigg[\sum_{k_1=4L-(J+4)}^{4L+1} S_6(k_1,4n-k_1-(J+3))\cdot A_{(L,k_1)}\cdot A_{(m,4n-k_1-(J+3))} + \sum_{k_1=4L-(J+3)}^{4L+1} S_7(k_1,4n-k_1-(J+2))\cdot A_{(L,k_1)}\cdot A_{(m,4n-k_1-(J+2))} + \sum_{k_1=4L-(J+2)}^{4L+1} S_8(k_1,4n-k_1-(J+1))\cdot A_{(L,k_1)}\cdot A_{(m,4n-k_1-(J+1))} + \sum_{k_1=4L-(J+2)}^{4L+1} S_8(k_1,4n-k_1-(J+1))\cdot A_{(L,k_1)}\cdot A_{(m,4n-k_1-(J+1))} + \sum_{k_1=4L-(J+1)}^{4L+1} S_9(k_1,4n-k_1-J)\cdot A_{(L,k_1)}\cdot A_{(m,4n-k_1-J)} + \sum_{k_1=4L-J}^{4L+1} S_{10}(k_1,4n-k_1-(J-1))\cdot A_{(L,k_1)}\cdot A_{(m,4n-k_1-(J-1))}\Bigg]\right\}$$

where $m = n - L$ and J varies form $-5,-4,-3,-2,-1,0,1,\ldots(4n-2)$.

$$S_1(k) = (-2-2\gamma)(k+2)(k+1)k - 6(2+2\gamma)$$
$$S_2(k) = -2(-2-2\gamma)(k+1)k(k-1) + (4+6\gamma)(k+2)(k+1)k + 12(2+2\gamma)$$
$$S_3(k) = (-2-2\gamma)k(k-1)(k-2) - 2(4+2\gamma)(k+1)k(k-1) - 2(k+2)(k+1)k - 6(2+2\gamma)$$
$$S_4(k) = (4+2\gamma)k(k-1)(k-2) + 4(k+1)k(k-1)$$
$$S_5(k) = -2k(k-1)(k-2)$$

$$S_6(k_1,k_2) = (k_2+2)(k_2+1)k_2$$
$$S_7(k_1,k_2) = -2(k_2+1)k_2(k_2-1) - 2(k_2+2)(k_2+1)k_2$$
$$S_8(k_1,k_2) = 4(k_2+1)k_2(k_2-1) + k_2(k_2-1)(k_2-2) + (k_2+2)(k_2+1)k_2$$
$$S_9(k_1,k_2) = -2k_2(k_2-1)(k_2-2) - 2(k_2+1)k_2(k_2-1)$$
$$S_{10}(k_1,k_2) = k_2(k_2-1)(k_2-2)$$

The expression for axial velocity profile obtained in the form

$$H(\eta) = -2\eta + (4+2\gamma)\eta^2 - (2+2\gamma)\eta^3 + \sum_{n=1}^{\infty} R^n \sum_{k=2}^{4n+1} A_{(n,k)}\left[\eta^{(k+2)} - 2\eta^{(k+1)} + \eta^k\right]. \tag{3.31}$$

The shear stress at the wall is given by

$$H''(0) = (8+4\gamma) + 2\sum_{n=1}^{\infty} R^n \sum_{k=2}^{4n+1} A_{(n,k)}. \tag{3.32}$$

The universal coefficients of the above series (3.32) representing shear stress which are decreasing in magnitude but displays random sign patterns. The radius of the convergence of the series

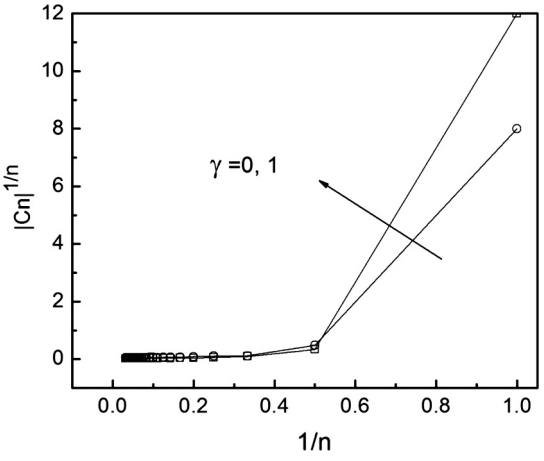

Fig. 2. Domb-Sykes plot for the series $H''(0)$ for different values of γ.

is obtained from Domb-Sykes plot (Fig. 2) for the stretching parameter $\gamma = 0$ and 1. Results are further extrapolated using rational approximation [63] for determining the radius of convergence. The Domb-Sykes plot (Fig. 2) after extrapolation, confirms the radius of convergence of the series to be $R_0 = 19.38991$ and 56.10381 for $\gamma = 0$ and 1 respectively for the series (3.32). The direct sum of the series for vertical and radial velocities is valid only up to the radius of convergence. The regions of the validity of the series are further increased by using the Pade' approximants.

4. Homotopy analysis method

4.1. Basic Idea of HAM

In general, Let us consider the nonlinear differential equation

$$\aleph[u(x) = 0 \tag{4.33}$$

where $\aleph$ is the nonlinear differential operator, x be the independent variable and $u(x)$ is the unknown function. By means of generalizing the traditional concept of homotopy Liao [45,64,65] constructed the following zeroth order deformation equation

$$(1-q)L[U(x,q) - u_0(x)] = q\hbar\aleph[U(x,q)] \tag{4.34}$$

where $q \in [0,1]$ is an embedding parameter, L is an auxiliary linear operator, $u_0(x)$ is an initial guess, $\hbar$ is the non-zero auxiliary parameter and $U(x)$ is an unknown function on the independent variable x and q.

For $q = 0$ and $q = 1$, then zeroth order deformation equation have the solutions respectively as

$$U(x,0) = u_0(x) \text{ and } U(x,1) = u(x) \tag{4.35}$$

As q vary from 0 to 1, $U(x,q)$ also vary from the initial guess $u_0(x)$ to the exact solution $u(x)$. Using the parameter q, we expand $U(x,q)$ in terms of Taylor's series as follows

$$U(x,q) = u_0(x) + \sum_{m=1}^{\infty} u_m(x) q^m \tag{4.36}$$

where $u_m(x) = \frac{1}{m!}\frac{\partial^m U(x,q)}{\partial q^m}\Big|_{q=0}$. Assume that the auxiliary linear operator, the initial guess, the auxiliary function are selected in such a way that the series (4.36) is convergent at $q = 1$, we have

$$u(x,q) = u_0(x) + \sum_{m=1}^{\infty} u_m \tag{4.37}$$

Differentiating the zeroth order deformation problem (4.34) 'm' times with respect to q then dividing it by $m!$ and finally setting $q = 0$. The resulting mth-order deformation equation becomes

$$L[u_m(x) - \chi_m u_{m-1}(x)] = \hbar H(x)\Re_m(u_{m-1}) \tag{4.38}$$

where

$$\Re_m(u_{m-1}) = \frac{1}{(m-1!)}\frac{\partial^{m-1}\aleph[u(x,q)]}{\partial q^{m-1}}\Big|_{q=0} \tag{4.39}$$

and

$$\chi_m = \begin{cases} 0, & m \leqslant 1; \\ 1, & m > 1; \end{cases} \tag{4.40}$$

To solve the linear system of equations (4.34) with the homogeneous boundary conditions up to any order of approximations. In this paper we used the Mathematica software for solving the flow problem.

4.2. Solution for problem

We seek the HAM solution of Eq. (2.11) subjected to the boundary conditions (2.10). We choose the initial guess which satisfies the boundary conditions automatically and auxiliary linear operator as

$$H_0(\eta) = -2\eta + (4+2\gamma)\eta^2 - (2+2\gamma)\eta^3 \tag{4.41}$$

and

$$L[H] = H^{IV} \tag{4.42}$$

The linear operator satisfy the below property

$$L\left[C_1\frac{\eta^3}{6} + C_1\frac{\eta^2}{2} + C_3\eta + C_4\right] = 0 \tag{4.43}$$

where C_1, C_2, C_3 and C_4 are arbitrary constants.

If $q \in [0,1]$ then the zeroth order deformation problem can be constructed as

$$(1-q)L[H(\eta,q) - H_0(\eta)] = q\hbar\aleph[H(\eta,q)] \tag{4.44}$$

also the boundary conditions becomes

$$H(0,q) = 0, \quad H(1,q) = 0, \quad H'(0,q) = -2, \quad H'(1,q) = -2\gamma. \tag{4.45}$$

where $q \in [0,1]$ is an embedding parameter, $\hbar$ and H are the non-zero auxiliary parameter and auxiliary function respectively. Further $\aleph$ is the non-linear differential operator and is given by

$$\aleph[H(\eta,q)] = \frac{\partial^4 H(\eta,q)}{\partial\eta^4} - RH(\eta,q)\frac{\partial^3 H(\eta,q)}{\partial\eta^3} \tag{4.46}$$

For $q = 0$ and $q = 1$, Eq. (4.44) have the solutions respectively

$$H(\eta,0) = H_0(\eta) \text{ and } H(\eta,1) = H(\eta) \tag{4.47}$$

As q vary from 0 to 1, $H(\eta,q)$ also vary from the initial guess $H_0(\eta)$ to the exact (final) solution $H(\eta)$. By Taylor's theorem, Eq. (4.47) can be written as

$$H(\eta,q) = H_0(\eta) + \sum_{m=1}^{\infty} H_m(\eta) q^m \tag{4.48}$$

where $H_m(\eta) = \frac{1}{m!}\frac{\partial^m H(\eta,q)}{\partial q^m}\Big|_{q=0}$. The convergence of the series (4.48) depends on the auxiliary parameter $\hbar$. To select the value of $\hbar$ in such a way that the series (4.48) is convergent at $q = 1$, we have

$$H(\eta,q) = H_0(\eta) + \sum_{m=1}^{\infty} H_m(\eta) \tag{4.49}$$

Differentiating the zeroth order deformation problem (4.44) 'm' times with respect to q and finally setting $q = 0$. The resulting mth-order deformation problem becomes

$$L[H_m(\eta) - \chi_m H_{m-1}(\eta)] = \hbar\Re_m(\eta) \tag{4.50}$$

and the homogeneous boundary conditions are

$$H_m(0) = 0, \quad H_m(1) = 0, \quad H'_m(0) = 0, \quad H'_m(1) = 0, \tag{4.51}$$

where

$$\Re_m(\eta) = H'''_{m-1} + R\sum_{n=0}^{m-1}[H_n H'''_{m-1-n}]. \tag{4.52}$$

and

$$\chi_m = \begin{cases} 0, & m \leqslant 1; \\ 1, & m > 1; \end{cases} \tag{4.53}$$

We use Mathematica to solve the linear system of equations (4.50) with the appropriate homogeneous boundary conditions (4.51) up to first few orders of approximations

Please cite this article in press as: V.B. Awati et al., Series analysis for the flow between two stretchable disks, Eng. Sci. Tech., Int. J. (2016), http://dx.doi.org/10.1016/j.jestch.2016.11.011

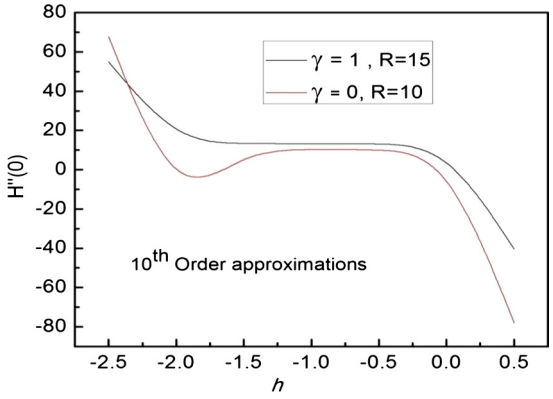

Fig. 3. $\hbar$ curves for the series $H''(0)$ for different values of γ and R.

$$H_1 = \hbar R\left[\frac{1}{35}(-4-\gamma+3\gamma^2)\eta^2+\frac{1}{105}(22+9\gamma-13\gamma^2)\eta^3 + \left(-\frac{1}{5}-\frac{\gamma}{5}\right)\eta^5+\frac{1}{15}(2+3\gamma+\gamma^2)\eta^6+\frac{1}{35}(-1-2\gamma-\gamma^2)\eta^7\right] \quad (4.54)$$

$$\begin{aligned} H_2 = &-\frac{-\hbar R}{727650}(-1+\eta)^2\eta^2(1+\gamma)(6930(12+\eta(2-5\gamma) \\ &-9\gamma+3\eta^3(1+\gamma)-\eta^2(8+\gamma))+\hbar(6930(12+\eta(2-5\gamma) \\ &-9\gamma+3\eta^3(1+\gamma)-\eta^2(8+\gamma))+R(1134\eta^7(1+\gamma)^2 \\ &+\eta(2570-1867-202\gamma^2)-378\eta^6(16+21\gamma+5\gamma^2) \\ &-7\eta^4(826-515\gamma+34\gamma^2)-14\eta^5(818-464\gamma+76\gamma^2) \\ &-6(83-373\gamma+314\gamma^2)+6\eta^3(-1090-178\gamma+527\gamma^2) \\ &+2\eta^2(2819-2986\gamma+740\gamma^2)))) \end{aligned}$$

4.3. Convergence of HAM

The series (4.48) contains the auxiliary parameter $\hbar$ and the convergence of the series strictly depends upon the value of parameter $\hbar$ which is known as convergence control parameter. This parameter plays an important role in determining the convergence region and rate of approximation for the HAM solutions. To obtain the permissible ranges of the parameter $\hbar$, draw the line segment of the $\hbar$ curves parallel to η-axis. Fig. 3 shows the $\hbar$ curves for the series $H''(0)$ for different values of R at the 10th order of approximations, it clearly indicates that the admissible ranges of $\hbar$ are $-1.25 \leqslant \hbar \leqslant -0.25$ and $-1.5 \leqslant \hbar \leqslant -0.25$ for $\gamma = 0$ and 1 respectively. In order to obtain the suitable value for $\hbar$, the $\hbar$ curve for residual error [50–52,66] of f is plotted in Fig. 3a. From this range, the HAM results are obtained up to 5th decimal places correctly. Our computation depicts that the series converges in the whole region of η when $\hbar = -1$. Also Table 2 presents the convergence analysis of the series solutions for shear stress for various orders of approximations. It is observed that the convergence is attained for the function $H''(0)$ at 30th order of approximation and it is enough to calculate the driveled quantities.

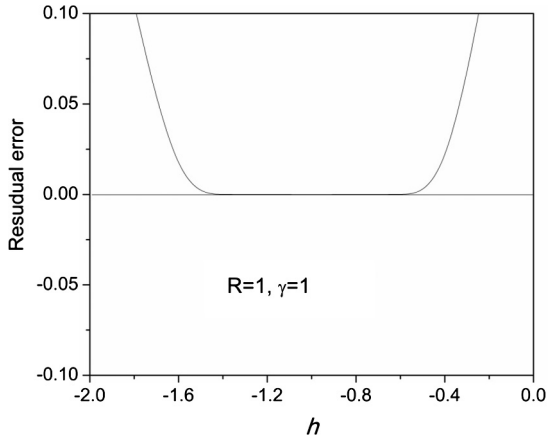

Fig. 3a. Residual error for h for the function f when $R = 1$ and $\gamma = 1$.

Table 2
Convergence of HAM solutions for increasing order of approximations for $R = 10$ and $\gamma = 10$.

Order of approximations	$H''(0)$
5	09.142857
10	10.262188
15	10.316786
20	10.317959
25	10.317990
30	10.317991
35	10.317991
40	10.317991

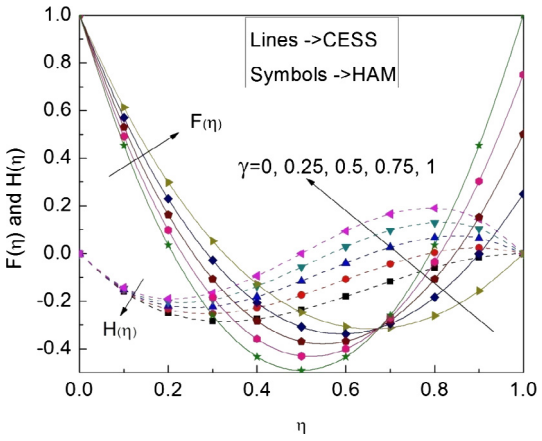

Fig. 4. Radial and vertical velocity profiles for different stretching parameter for $R = 2$.

5. Results and discussions

The equation of motion for the fluid flow is governed by nonlinear ODE (2.11) together with the boundary conditions (2.10) are solved by CESS, Dirichlet series and HAM. A new type of series expansion scheme with universal polynomial coefficients proposed here enables in deriving a recurrence relation, which generates large number of universal polynomial coefficients $A_{(n,k)}, k = 2,3,\ldots 4n+1$ and $n = 1,2,\ldots,31$. These coefficients in turn give universal polynomial functions $H_n(\eta), n = 1,2,\ldots,31$. The series (3.31) representing velocity profiles can be analyzed by using Pade' approximants for much larger values of Reynolds number for different stretching parameters (γ). The velocity profiles are shown in Figs 3 and 4, which are found to be identical with the HAM curves for different values of Reynolds number and γ. The coefficients of the series (3.32) representing shear stress for different values of the stretching parameter γ have random sign patterns and decrease in magnitude. Fig. 2 shows the Domb-Sykes plot, which estimates the location and identify the nature of the nearest singularity which restricting the convergence region. The rational extrapolation yields the radius of convergence of the series (3.32) to be $R_0 = 19.38991$ and 56.10381 for $\gamma = 0$ and 1 respectively.

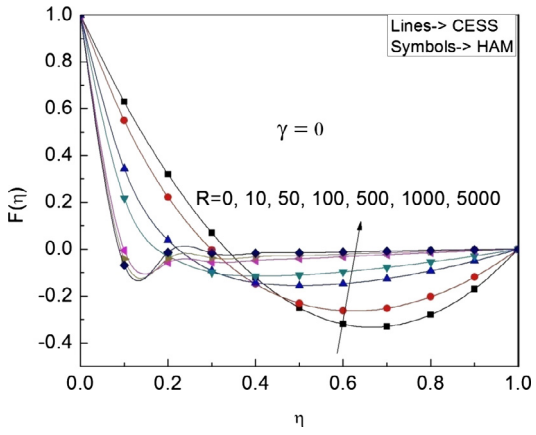

Fig. 5a. The velocity profiles for $\gamma = 0$ as a function of R.

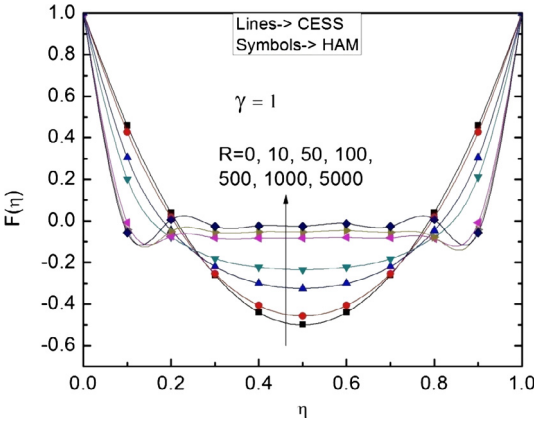

Fig. 5b. The velocity profiles for $\gamma = 1$ as a function of R.

The direct sum of the series (3.32) is valid only up to the radius of convergence. We use Pade' approximants [67] for summing the series which give a converging sum for much larger values of Reynolds number up to ∞.

The velocity profiles are shown in Fig. 4 for different values of wall stretching parameters γ with $R = 2$. It is observed that the radial velocity near the wall is stretched by the wall movement. However, away from the wall there exists a negative radial flow to balance the mass stretched out by the wall to be consistent for the force balance. In the radial direction the fluid is stretched along the wall with outer flow near the right side wall for non-zero stretching parameter. Due to the wall stretching the vertical velocity is downward near the left wall. As we seen, the negative velocity profiles dominant for stretching parameters less than one, the overall net flow rate is downward.

The net flow along the vertical direction is zero due to a symmetric stretching for $\gamma = 1$. In the vertical direction the maximum negative velocity decreases with the increase of stretching parameter while in the radial direction there occurs a larger maximum negative velocity for symmetric stretching disks.

The radial velocity profiles are shown in Fig. 5a for various Reynolds number with asymmetric stretching parameter $\gamma = 0$. It is seen that the velocity profiles become closer to the left wall and also the maximum negative velocity decreases with the increase of R. The radial velocity profiles are presented in Fig. 5b for different values of R for symmetric stretching parameter $\gamma = 1$, by increasing Reynolds number the boundary layer flow becomes more obvious. There is an inviscid core flow in the central part between the two stretchable disks. It is observed that the velocity profiles become closer to both the walls and also the maximum negative velocity decreases in the central region with the increase of R. From the Figs. 5a and 5b, the profiles shows a creeping flow behavior with parabolic in nature when the Reynolds number $R = 0$.

The wall shear stress $H''(0)$ profiles are given in Fig. 6 for different values of γ as a function of Reynolds number R. It is observed that the shear stress values increases with the increasing function of R. For small as well as large Reynolds numbers Eq. (3.32) provides a good prediction of $H''(0)$. The pressure parameter profiles

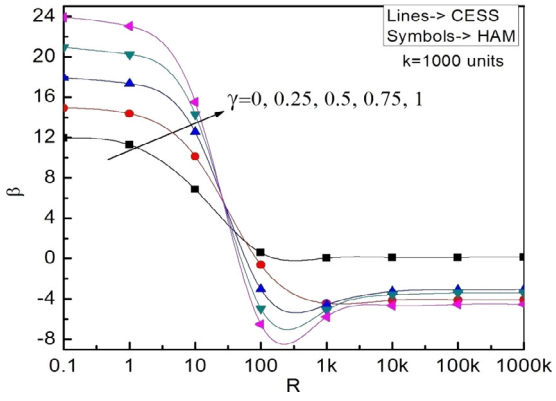

Fig. 7. The pressure parameter β for different values of γ as a function of R.

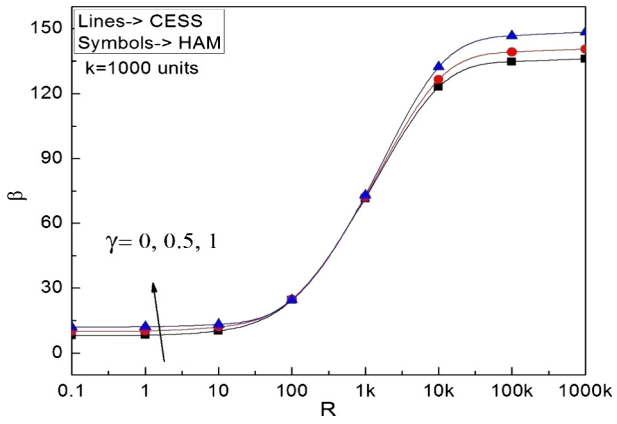

Fig. 6. The shear stress profiles for different values of γ as a function of R.

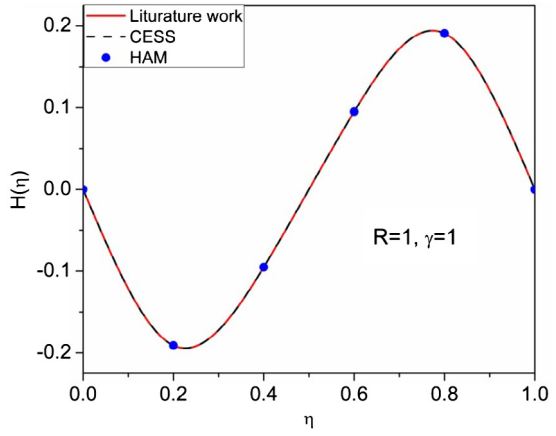

Fig. 8. Comparison of present velocity profiles with literature results [61] for $R = 1$ and $\gamma = 1$.

are shown in Fig. 7 for different values of γ as a function of R. The β value decreases with the increase of R and finally approaches towards zero for very large R, when $\gamma = 0$. But for non-zero values of γ, the pressure parameter β falls to a negative value and reaches a minimum point, then it is little bit increases and lastly approaches to a negative value depending on γ. For the symmetric stretching case ($\gamma = 1$), we obtain the value of $\beta \to -4.521794$, when $R \to \infty$. The pressure parameter β results are compared with CESS and HAM is a benchmark against numerical solution [61], thus the results are presented in the form of graphs.

To check the validity of our present (CESS and HAM) velocity profiles, the comparison is made with the earlier literature work [61]. The obtained results are in good agreements which are presented through the graphs as shown in the Fig. 8.

6. Conclusion

In this paper, we analyze the boundary value problem arises in the axis-symmetric flow between two coaxial infinite stretching disks by using series methods viz. CESS, Dirichlet series and HAM. Also, we have given the recurrence relation for generating the unknown coefficients in terms of polynomial functions in the series. To analyze the validity of convergence, we identified and estimated the location and nature of the singularities restrict the convergence of the series which can be predicted by using Domb-Sykes plot. The effects of disk stretching parameter γ and wall stretching Reynolds number R were discussed in detail through graphs. By increasing the Reynolds numbers, the viscous fluid begins with a creeping flow at $R = 0$ to a typical boundary layer flow for large Reynolds numbers. The wall shear stress increases with the increasing function of R for different values of γ. The pressure parameter falls from higher to lower values with increasing Reynolds number for non-zero γ. The validity of the series solution is extended to a much larger values of R up to infinity by using analytic continuation. The comparisons of result are in excellent agreement between series solution and numerical solution.

References

[1] T. Altan, S. Oh, H. Gegel, Metal Forming Fundamentals and Applications, American Society for Metals, Metals Park, OH, 1983.
[2] E.G. Fisher, Extrusion of Plastics, Wiley, New York, 1976.
[3] Z. Tadmor, I. Klein, Engineering Principles of Plasticating Extrusion, Van Nostrand Reinhold, New York, 1970.
[4] B.C. Sakiadis, Boundary layer behavior on continuous solid surfaces: I. Boundary-layer equations for two-dimensional and axisymmetric flow, AICHE J. 7 (1961) 26–28.
[5] B.C. Sakiadis, Boundary layer behavior on continuous solid surfaces: II. The boundary layer on a continuous flat surface, AICHE J. 7 (1961) 221–225.
[6] C.Y. Wang, Exact solutions of the steady-state Navier-Stokes equations, Annu. Rev. Fluid Mech. 23 (1) (1991) 159–177.
[7] L.J. Crane, Flow past a stretching plate, J. Appl. Math. Phys. 21 (1970) 645–647.
[8] H.K. Kuiken, On boundary layers in fluid mechanics that decay algebraically along stretches of wall that are not vanishingly small, IMA J. Appl. Math. 27 (1981) 387–405.
[9] W.H.H. Banks, Similarity solutions of the boundary layer equations for a stretching wall, J. Mec. Theor. Appl. 2 (1983) 375–392.
[10] P.S. Gupta, A.S. Gupta, Heat and mass transfer on a stretching sheet with suction or blowing, Can. J. Chem. Eng. 55 (1977) 744–746.
[11] C.Y. Wang, Stretching surface in a rotating fluid, J. Appl. Math. Phys. (ZAMP) 39 (1988) 177–185.
[12] C.Y. Wang, The three dimensional flow due to a stretching flat surface, Phys. Fluids 27 (1984) 1915–1917.
[13] J.F. Brady, A. Acrivos, Steady flow in a channel or tube with an accelerating surface velocity. An exact solution to the Navier-Stokes equations with reverse flow, J. Fluid Mech. 112 (1981) 127–150.
[14] C.Y. Wang, Fluid flow due to a stretching cylinder, Phys. Fluids 31 (1988) 466–468.
[15] E.B.B. Watson, W.H.H. Banks, M.B. Zatuska, P.G. Drazin, On transition to chaos in two-dimensional channel flow symmetrically driven by accelerating walls, J. Fluid. Mech. 212 (1990) 451–485.
[16] P. Watson, W.H.H. Banks, M.B. Zaturska, P.G. Drazin, Laminar channel flow driven by accelerating walls, Eur. J. Appl. Math. 2 (1991) 359–385.
[17] M.B. Zaturska, W.H.H. Banks, Flow in a pipe driven by suction at an accelerating wall, Acta Mech. 110 (1995) 111–121.
[18] L. Durlofsky, J.F. Brady, The spatial stability of a class of similarity solutions, Phys. Fluids 27 (1984) 1068–1076.
[19] M.B. Zaturska, W.H.H. Banks, New solutions for flow in a channel with porous walls and/or non-rigid walls, Fluid Dyn. Res. 33 (2003) 57–71.
[20] H. Rasmussen, Steady viscous flow between two porous disks, Z. Angew. Math. Phys. 21 (1970) 187–195.
[21] M. Turkyilmazoglu, MHD fluid flow and heat transfer due to a stretching rotating disk, Int. J. Therm. Sci. 51 (2012) 195–201.
[22] M. Turkyilmazoglu, Three dimensional MHD stagnation flow due to a stretchable rotating disk, Int. J. Heat Mass Transfer 55 (2012) 6959–6965.
[23] M. Turkyilmazoglu, Flow and heat simultaneously induced by two stretchable rotating disks, Phys. Fluids 28 (2016), http://dx.doi.org/10.1063/1.4945651.
[24] M. Mustafa, J. Ahmad Khan, T. Hayat, A. Alsaedi, On Bödewadt flow and heat transfer of nanofluids over a stretching stationary disk, J. Mol. Liquids 211 (2015) 119–125.
[25] M. Imtiaz, T. Hayat, A. Alsaedi, B. Ahmad, Convective flow of carbon nanotubes between rotating stretchable disks with thermal radiation effects, Int. J. Heat Mass Transfer 101 (2016) 948–957.
[26] T. Hayat, S. Qayyum, M. Imtiaz, F. Alzahrani, A. Alsaedi, Partial slip effect in flow of magnetite-Fe_3O_4 nanoparticles between rotating stretchable disks, J. Magn. Magn. Mater. 413 (2016) 39–48.
[27] T. Hayat, M. Imtiaz, A. Alsaedi, F. Alzahrani, Effects of homogeneous–heterogeneous reactions in flow of magnetite-Fe_3O_4 nanoparticles by a rotating disk, J. Mol. Liquids 216 (2016) 845–855.
[28] T. Hayat, M. Nawaz, Unsteady stagnation point flow of viscous fluid caused by an impulsively rotating disk, J. Taiwan Inst. Chem. Eng. 42 (2011) 41–49.
[29] M. Sheikholeslami, D.D. Ganji, Heat transfer of Cu-water nanofluid flow between parallel plates, Powder Technol. 235 (2013) 873–879.
[30] M. Sheikholeslami, H.R. Ashorynejad, D.D. Ganji, A. Kolahdooz, Investigation of rotating MHD Viscous Flow and Heat Transfer between Stretching and Porous Surfaces Using Analytical Method, Hindawi Publishing Corporation Math. Prob. Eng., 2011, 17 pages, http://dx.doi.org/10.1155/2011/258734.
[31] M. Sheikholeslami, H.R. Ashorynejad, D.D. Ganji, A. Yıldırım, Homotopy perturbation method for three-dimensional problem of condensation film on inclined rotating disk, Sci. Iran. B 19 (3) (2012) 437–442.
[32] M. Sheikholeslami, D.D. Ganji, M.M. Rashidi, Magnetic field effect on unsteady nanofluid flow and heat transfer using Buongiorno model, J. Magn. Magn. Mater. 416 (2016) 164–173.
[33] M. Sheikholeslami, D.D. Ganji, Nanofluid flow and heat transfer between parallel plates considering Brownian motion using DTM, Comput. Methods Appl. Mech. Eng. 283 (2015) 651–663.
[34] M. Sheikholeslami, R. Ellahi, H.R. Ashorynejad, G. Domairry, T. Hayat, Effects of heat transfer in flow of nanofluids over a permeable stretching wall in a porous medium, J. Comput. Theor. Nanosci. 1–11 (2014).
[35] M. Sheikholeslami, D.D. Ganji, H.R. Ashorynejad, Houman B. Rokni, Analytical investigation of Jeffery-Hamel flow with high magnetic field and nano particle by Adomian decomposition method, Appl. Math. Mech.-Engl. Ed. 33 (1) (2012) 1553–1564.
[36] M. Sheikholeslami, D.D. Ganji, H.R. Ashorynejad, Investigation of squeezing unsteady nanofluid flow using ADM, Powder Technol. 239 (2013) 259–265.
[37] M. Sheikholeslami, D.D. Ganji, Magnetohydrodynamic flow in a permeable channel filled with nano fluid, Sci. Iran. B 21 (1) (2014) 203–212.
[38] M. Sheikholeslami, H.R. Ashorynejad, Davood Domairry, I. Hashim, Investigation of the laminar viscous flow in a semi-porous channel in the presence of uniform magnetic field using optimal homotopy asymptotic method, Sains Malaysiana 41 (10) (2012) 1177–1229.
[39] M. Van Dyke, Analysis and improvement of perturbation series, Q. J. Mech. 27 (1974) 423–450.
[40] V.B. Awati, N.M. Bujurke, N.N. Katagi, Computer extended series solution for the flows in a nonparallel channels, Adv. Appl. Sci. Res. 3 (4) (2012) 2413–2423.
[41] N.M. Bujurke, V.B. Awati, N.N. Katagi, Computer extended series solution for flow in a narrow channel of varying gap, Appl. Math. Comput. 186 (2007) 54–69.
[42] N.M. Bujurke, N.N. Katagi, V.B. Awati, Analysis of steady viscous flow in slender tubes, Z. Angew. Math. Phys. 56 (2005) 831–851.
[43] N.M. Bujurke, N.N. Katagi, V.B. Awati, Analysis of Laminar flow in a channel with one porous bounding wall, Int. J. Fluid Mech. Res. (IJFMR) 37 (3) (2010) 1–15.
[44] C. Domb, M.F. Sykes, On the susceptibility of a ferromagnetic above the curic point, Proc. Roy. Lond. Ser. A 240 (1957) 214–228.
[45] S. J. Liao, The proposed homotopy analysis technique for the solution of nonlinear problems, Ph.D Thesis, Shanghai Jiao Tong University. (1992).
[46] Vishwanath B. Awati, Manjunath Jyoti, N.N. Katagi, Computer extended series and homotopy analysis method for the solution of MHD flow of viscous fluid between two parallel porous plates, Gulf J. Math. 4 (2016) 65–79.
[47] T. Hayat, M. Imtiaz, A. Alsaedi, S. Almezal, On Cattaneo-Christov heat flux in MHD flow of Oldroyd-B fluid with homogeneous–heterogeneous reactions, J. Magn. Mag. Mater. 401 (2016) 296–303.

Please cite this article in press as: V.B. Awati et al., Series analysis for the flow between two stretchable disks, Eng. Sci. Tech., Int. J. (2016), http://dx.doi.org/10.1016/j.jestch.2016.11.011

[48] S. Abbasbandy, R. Naz, T. Hayat, A. Alsaedi, Numerical and analytical solutions for Falkner-Skan flow of MHD Maxwell fluid, AMC 242 (2014) 569–575.
[49] S.A. Shehzad, T. Hayat, A. Alsaedi, M.A. Obid, Nonlinear thermal radiation in three-dimensional flow of Jeffrey nanofluid: a model for solar energy, AMC 248 (2014) 273–286.
[50] T. Hayat, M. Imtiaz, A. Alsaedi, Melting heat transfer in the MHD flow of Cu–water nanofluid with viscous dissipation and Joule heating, Adv. Powder Technol. 27 (2016) 1301.
[51] T. Hayat, M. Ijaz Khan, M. Farooq, A. Alsaedi, M. Waqas, T. Yasmeen, Impact of Cattaneo-Christov heat flux model in flow of variable thermal conductivity fluid over a variable thicked surface, Int. J. Heat Mass Transfer 99 (2016) 702–710.
[52] T. Hayat, S. Qayyum, A. Alsaedi, Anum Shafiq, Inclined magnetic field and heat source/sink aspects in flow of nanofluid with nonlinear thermal radiation, Int. J. Heat Mass Transfer 103 (2016) 99–107.
[53] T. Hayat, S. Qayyum, M. Imtiaz, A. Alsaedi, Comparative study of silver and copper water nanofluids with mixed convection and nonlinear thermal radiation, Int. J. Heat Mass Transfer 102 (2016) 723–732.
[54] T. Hayat, A. Aziz, T. Muhammada, A. Alsaedib, On magnetohydrodynamic three-dimensional flow of nanofluid over a convectively heated nonlinear stretching surface, Int. J. Heat Mass Transfer 100 (2016) 566–572.
[55] T. Hayat, M. Imtiaz, A. Alsaedi, MHD 3D flow of nanofluid in presence of convective conditions, J. Mol. Liquids 212 (2015) 203–208.
[56] M. Imtiaz, T. Hayat, A. Alsaedi, A. Hobiny, Homogeneous-heterogeneous reactions in MHD flow due to an unsteady curved stretching surface, J. Mol. Liquids 221 (2016) 245–253, http://dx.doi.org/10.1016/j.molliq.2016.05.060.
[57] T. Hayat, M. Waqas, S. Ali Shehzad, A. Alsaedi, On model of Burgers fluid subject to magneto nanoparticles and convective conditions, J. Mol. Liquids 222 (2016) 181–187.
[58] M. Farooq, M. Ijaz Khan, M. Waqas, T. Hayat, A. Alsaedi, M. Imran Khan, MHD stagnation point flow of viscoelastic nanofluid with non-linear radiation effects, J. Mol. Liquids 221 (2016) 1097–1103.
[59] T. Hayat, M. Ijaz Khan, M. Farooq, T. Yasmeen, A. Alsaedi, Stagnation point flow with Cattaneo-Christov heat flux and homogeneous-heterogeneous reactions, J. Mol. Liquids 220 (2016) 49–55.
[60] F.M. White, Viscous Fluid Flow, 2nd ed., McGraw-Hill Company, New York, 1991.
[61] T. Fang, J. Zhang, Flow between two stretchable disks – an exact solution of the Navier-Stokes equations, Int. Commun. Heat Mass Transfer 35 (2008) 892–895.
[62] S. Riesz, Introduction to Dirichlet Series, Camb. Univ, Press, 1957.
[63] W.H. Press, S.A. Flannery, Teukolsky, W.T. Vetterling, Numerical Recipes, Cambridge University Press, 1986.
[64] S.J. Liao, Beyond Perturbation: Introduction to Homotopy Analysis Method, Chapman & Hall/CRC Press, Boca Raton, 2003.
[65] S.J. Liao, Homotopy Analysis Method in Nonlinear Differential Equations, Higher Education Press, Beijing and Springer-Verlag, Berlin Heidelberg, 2012.
[66] M. Turkyilmazoglu, An effective approach for evaluation of the optimal convergence control parameter in the homotopy analysis method, Filomat 30 (2016) 1633–1650.
[67] C.M. Bender, S.A. Orszag, Advanced Mathematical Methods for Scientists and Engineers, 3rd International ed., Mc-Grawhill Book Company, New York, 1987.

Please cite this article in press as: V.B. Awati et al., Series analysis for the flow between two stretchable disks, Eng. Sci. Tech., Int. J. (2016), http://dx.doi.org/10.1016/j.jestch.2016.11.011